A Yeast Heterogeneous Nuclear Ribonucleoprotein Complex Associated With RNA Polymerase II

Nicholas K. Conrad,* Scott M. Wilson,†,1 Eric J. Steinmetz,‡ Meera Patturajan,*,2 David A. Brow,‡ Maurice S. Swanson† and Jeffry L. Corden*

**Department of Molecular Biology and Genetics, The Johns Hopkins University School of Medicine, Baltimore, Maryland 21205,* †*Department of Molecular Genetics and Microbiology and Centers for Gene Therapy and Mammalian Genetics, College of Medicine, University of Florida, Gainsville, Florida 32610 and the* ‡*Department of Biomolecular Chemistry, University of Wisconsin Medical School, Madison, Wisconsin 53706*

Manuscript received July 23, 1999
Accepted for publication October 12, 1999

ABSTRACT

Recent evidence suggests a role for the carboxyl-terminal domain (CTD) of the largest subunit of RNA polymerase II (pol II) in pre-mRNA processing. The yeast *NRD1* gene encodes an essential RNA-binding protein that shares homology with mammalian CTD-binding proteins and is thought to regulate mRNA abundance by binding to a specific *cis*-acting element. The present work demonstrates genetic and physical interactions among Nrd1p, the pol II CTD, Nab3p, and the CTD kinase CTDK-I. Previous studies have shown that Nrd1p associates with the CTD of pol II in yeast two-hybrid assays via its CTD-interaction domain (CID). We show that *nrd1* temperature-sensitive alleles are synthetically lethal with truncation of the CTD to 9 or 10 repeats. Nab3p, a yeast hnRNP, is a high-copy suppressor of some *nrd1* temperature-sensitive alleles, interacts with Nrd1p in a yeast two-hybrid assay, and coimmunoprecipitates with Nrd1p. Temperature-sensitive alleles of *NAB3* are suppressed by deletion of *CTK1*, a kinase that has been shown to phosphorylate the CTD and increase elongation efficiency *in vitro*. This set of genetic and physical interactions suggests a role for yeast RNA-binding proteins in transcriptional regulation.

EUKARYOTIC messenger RNA biogenesis is a complex, multistep process carried out by molecular machines consisting of hundreds of polypeptides. While many components of the transcription and splicing machines have been identified and assigned functional roles, less is known about how the synthesis of pre-mRNA is synchronized with its processing and transport. As nascent pre-mRNA emerges from the elongating RNA polymerase II (pol II), its postsynthetic fate is determined by a large number of RNA-binding proteins. Primary among these proteins are the heterogeneous nuclear ribonucleoproteins (hnRNPs) that have been shown to play multiple roles in processing and transport (Siomi and Dreyfuss 1997; Krecic and Swanson 1999). These proteins are thought to be the first to bind nascent transcripts, but how, or indeed whether, they interact with the transcription machinery as RNA-bound factors has not been investigated previously.

Recent studies have indicated that the carboxyl-terminal domain (CTD) of the largest subunit of pol II interacts with multiple pre-mRNA processing components. Direct interaction between the CTD and capping (Cho *et al.* 1997, 1998; McCracken *et al.* 1997a; Yue *et al.* 1997; Ho *et al.* 1998; Ho and Shuman 1999; Pillutla *et al.* 1998) and 3′-end processing (McCracken *et al.* 1997b) components has been demonstrated. A highly phosphorylated form of pol II associates with spliceosome components (Mortillaro *et al.* 1996; Yuryev *et al.* 1996; Kim *et al.* 1997), and transcripts synthesized by pol II containing a deleted CTD are poorly spliced *in vivo* (McCracken *et al.* 1997b). The CTD is necessary for recruitment of pre-mRNA splicing factors to transcription sites *in vivo* (Misteli and Spector 1999). *In vitro*, a purified pol II complex with a hyperphosphorylated CTD stimulates splicing (Hirose *et al.* 1999), and 3′ processing can be stimulated by recombinant phosphorylated CTD (Hirose and Manley 1998). A recently identified set of serine-arginine (SR)-rich proteins termed SCAFs (*S*R-like *C*TD-*a*ssociated *f*actors, Yuryev *et al.* 1996; Corden and Patturajan 1997) can interact with the phosphorylated CTD (Patturajan *et al.* 1998b). These proteins are excellent candidates for coupling transcription and pre-mRNA processing.

The yeast *NRD1* gene encodes a protein with homology to mammalian SCAF8 and SCAF4 (Steinmetz and Brow 1996, 1998; Steinmetz 1997; Yuryev *et al.* 1996). These proteins all contain an N-terminal CTD-interacting domain (CID), a single RNA recognition motif

Corresponding author: Jeffry L. Corden, Department of Molecular Biology and Genetics, The Johns Hopkins University School of Medicine, 725 N. Wolfe St., Baltimore, MD 21205.
E-mail: jcorden@jhmi.edu

[1] *Present address:* Mammalian Genetics Laboratory, ABL-Basic Research Program, National Cancer Institute-Frederick Cancer Research and Development Center, Frederick, MD 21702.

[2] *Present address:* Department of Otolaryngology, The Johns Hopkins University School of Medicine, Baltimore, MD 21205.

(RRM), and a region rich in alternating charged residues (Corden and Patturajan 1997). In the mammalian proteins, the latter region is comprised mainly of alternating (phospho) serine and arginine residues similar to the SR protein family (Fu 1995). The yeast Nrd1p RE/RS motif contains relatively few arg/ser dipeptides, but is rich in arg/glu dipeptides.

NRD1 was identified originally as a gene encoding an hnRNP that mediated the downregulation of a reporter gene containing an exogenous sequence element in its intron (Steinmetz and Brow 1996). This artificial *cis*-acting RNA sequence, designated U6R*, comprises 112 bases derived from an antisense U6 RNA gene together with unrelated 5′ flanking sequences. The C-terminal portion of Nrd1p, containing the RRM, binds specifically to this RNA element *in vitro* (Steinmetz and Brow 1998). *In vivo*, truncated reporter RNA species with 3′ ends mapping to the U6R* element further suggest that Nrd1p plays a role in transcript elongation, termination, and/or 3′-end formation (Steinmetz 1997). The evolutionarily conserved N-terminal domain of Nrd1p interacts with the pol II CTD in a two-hybrid assay (Yuryev *et al.* 1996). More recent studies have shown that the mammalian SCAF8-CTD interaction is dependent on CTD phosphorylation (Patturajan *et al.* 1998b). Interaction with the phosphorylated CTD would place Nrd1p in transcription elongation complexes where it could monitor nascent transcripts for the presence of RNA signal sequences leading to 3′-end formation. Consistent with this model, deletion of most of the CTD-interacting domain eliminates Nrd1p-dependent downregulation of U6R*-containing pre-mRNA (Steinmetz and Brow 1998).

While *NRD1* is an essential gene, the CTD-interacting domain is not required for viability (Steinmetz and Brow 1998). To further investigate the essential cellular function of *NRD1*, we have isolated and characterized a set of temperature-sensitive *nrd1* mutants. We show here that several *nrd1* temperature-sensitive alleles are synthetically lethal with several CTD truncation mutations. In addition, we show that overexpression of another hnRNP, Nab3p, suppresses some *nrd1* temperature-sensitive alleles. A genome-wide two-hybrid screen with Nrd1p as bait yielded Nab3p as an interacting protein, and the region of Nrd1p necessary for interaction with Nab3p was mapped to <100 amino acid residues between the CID and RE/RS domains. Finally, we show that a *nab3* temperature-sensitive mutant is suppressed by a mutation in *CTK1*, a gene encoding the catalytic subunit of a kinase that phosphorylates the CTD. Together, these results suggest that the pol II CTD, Nrd1p, Nab3p, and the CTD kinase CTDK-I function together at the interface between transcription and pre-mRNA processing.

MATERIALS AND METHODS

Yeast strains, genetic methods, and media: *Saccharomyces cerevisiae* strains used in this study are listed in Table 1. BY4743, a derivative of S288C produced by mating BY4741 and BY4742 (Brachmann *et al.* 1998), is the parent of strains used in all *nrd1* domain deletion and temperature-sensitive experiments except for the CTD synthetic lethality analysis. The latter used ZAYA, which was derived from the mating of Z26 (Nonet *et al.* 1987) with AYA1 (Yuryev and Corden 1996). *NRD1* was targeted for disruption using a fragment generated by PCR of pUG6 with oligos JC827 (5′-AAAGG AACCG GAAAG CAACA AACAT ACTAA ACATC CCATA CCAGC TGAAG CTTCG TACGC-3′) and JC828 (5′-TTTTA TGTAC TATGA GCAAA TAAAG GGTGG AGTAA AGATC GCATA GGCCA CTAGT GGATC TG-3′), which amplified a product encoding a *Kan*^{r} gene flanked by 40 bp of homology to sequences upstream and downstream of *NRD1* coding sequence (Guldener *et al.* 1996). After transformation of the diploid strain and selection for Kan^r, disruption was confirmed via Southern blot, and sporulation verified that *NRD1* is essential in the background. Diploids were further transformed with a *URA3*-marked plasmid (pNRD-HA) encoding an epitope-tagged wild-type *NRD1* gene and sporulated, and the derived Kan^r/Ura$^+$ strains (YJC582 and YJC546) were used for subsequent experiments. Derivatives of these strains were made via transformation and counterselection on 0.1% 5-fluoroorotic acid (5-FOA) (Boeke *et al.* 1984).

Domain deletion analysis was carried out by transforming YJC582 with deletion constructs and retaining selection for both wild-type and deletion plasmids. Multiple independent transformants were grown to stationary phase in CSM-Leu-Ura. Dilution series were made (eightfold) and plated onto CSM-Leu 5-FOA plates at 15, 20, 25, 30, and 37°.

Rich (YPD) and minimal media used were prepared as described (Rose *et al.* 1990), except CSM dropout mix was obtained from Bio 101 (Vista, CA). Transformation of yeast was performed in lithium acetate as described (Schiestl and Gietz 1989).

Plasmids: Plasmids used in this study are summarized in Table 2. Most of the constructs generated in the present study used the pRS series of shuttle vectors (Sikorski and Hieter 1989; Christianson *et al.* 1992). All *NRD1* constructs in this study are derived from an ~5-kb genomic *Hin*dIII fragment containing the entire *NRD1* coding sequence and 1 kb of upstream sequence in pRS316 (Steinmetz and Brow 1996). Plasmid pNrd4 was created by subcloning the *Hin*dIII fragment into the *Hin*dIII site of pRS426 in the orientation that places the upstream sequence nearest the *Xho*I site of the vector. To remove ~2 kb of downstream sequence and engineer a *Not*I site at the termination codon of *NRD1*, PCR products using pNrd4 as template and primers JC811 (5′-GACCC CACTG CTCAA TT GAA TTCTT-3′), which includes an endogenous *Eco*RI site, and JC813 (5′-TTA GCGGCCGC TTTGT TGTTG TTGC-3′), which includes the engineered *Not*I terminator, were mixed with amplification products of pNrd4 with JC810 (5′-CCGCGAGCTCA AAGTT TATTG ATTGT TTAAC TG-3′) and JC812 (5′-AGCGGCCGCTA AGATCT TTACT CCA-3′). The latter products include the same *Not*I site (12-bp overlap) and ~280 bp of 3′ sequence. Relevant restriction sites in the primers are underlined. The mixed PCR products were used as a template for PCR with primers JC811/JC810, and the resulting fragment was cut with *Eco*RI and *Sac*I and ligated to *Eco*RI/*Sac*I-digested pNrd4. The resulting clone, pNrd1-Not, and all other constructs made via PCR were sequenced to exclude the possibility of PCR-induced mutations.

We tagged *NRD1* using the method of Tyers *et al.* (1992). An attempt to produce a triple-HA-tagged version of *NRD1* produced instead a double-tagged version of *NRD1* with a fortuitous termination codon following the internal *Bam*HI site (pNRD1-HA). Plasmids pJC504 and pJC580 were produced by transfer of *Xho*I/*Sac*I pNRD1-HA fragment to *Xho*I/*Sac*I-digested pRS414 and pRS415, respectively.

TABLE 1

Yeast strains used in this study

Name	Genotype
BY4743[a]	*MAT***a**/*MATα ura3Δ0/ura3Δ0 his3Δ1/his3Δ1 leu2Δ0/leu2Δ0 MET15/met15Δ0 LYS2/lys2Δ0*
YJC582	*MATα ura3Δ0 his3Δ1 leu2Δ0 met15Δ0 LYS2 nrd1Δ::KAN* (pNRD-HA2 [*URA3 NRD1-HA*])
YJC610	*MATα ura3Δ0 his3Δ1 leu2Δ0 met15Δ0 LYS2 nrd1Δ::KAN* (pJC580 [*LEU2 NRD1-HA*])
YJC818	*MATα ura3Δ0 his3Δ1 leu2Δ0 met15Δ0 LYS2 nrd1Δ::KAN* (pJC951 [*LEU2 nrd1-51*])
YJC824	*MATα ura3Δ0 his3Δ1 leu2Δ0 met15Δ0 LYS2 nrd1Δ::KAN* (pJC955 [*LEU2 nrd1-60*])
YJC1103	*MATα ura3Δ0 his3Δ1 leu2Δ0 met15Δ0 LYS2 nrd1Δ::KAN* (pJC719 [*LEU2 nrd1-101*])
YJC1107	*MATα ura3Δ0 his3Δ1 leu2Δ0 met15Δ0 LYS2 nrd1Δ::KAN* (pJC720 [*LEU2 nrd1-102*)
Z26[b]	*MATα ura3-52 his3-Δ200 leu2-3,112 rpb1-Δ187::HIS3* (pRP112 [*URA3 RPB1*])
AYA1[c]	*MAT***a** *ura3-52 his3-Δ200 leu2-3,112 rpb1-Δ187::HIS3 trp1-Δ63 cyh*^{R}*, can*^{R} (pY1At [*LEU2 RPB1*])
ZAYA	*MAT***a**/*MATα ura3-52/ura3-52 his3-Δ200/his3-Δ200 leu2-3,112/leu2-3,112 rpb1-Δ187::HIS3/112 rpb1-Δ187::HIS3 TRP1/trp1-Δ63* (pY1At [*LEU2 RPB1*], pRP112 [*URA3 RPB1*])
YJC546	*MATα ura3-52 his3-Δ200 leu2-3,112 rpb1-Δ187::HIS3 trp1-Δ63 nrd1Δ::KAN* (pY1At [*LEU2 RPB1*], pNRD1-HA [*URA3, NRD1-HA*])
YJC1111	*MATα ura3-52 his3-Δ200 leu2-3,112 rpb1-Δ187::HIS3 trp1-Δ63 nrd1Δ::KAN* (pRP112 [*URA3 RPB1*], pJC504 [*TRP1 NRD1-HA*])
YJC1115	*MATα ura3-52 his3-Δ200 leu2-3,112 rpb1-Δ187::HIS3 trp1-Δ63 nrd1Δ::KAN* (pRP112 [*URA3 RPB1*], pJC705 [*TRP1 nrd1-51*])
YJC1119	*MATα ura3-52 his3-Δ200 leu2-3,112 rpb1-Δ187::HIS3 trp1-Δ63 nrd1Δ::KAN* (pRP112 [*URA3 RPB1*], pJC710 [*TRP1 nrd1-83*])
PJ69-4A[d]	*MAT***a** *trp1-901 leu2-3, 112 ura3-52 his3-200 gal4Δ gal80Δ LYS2::GAL1-HIS3 GAL2-ADE2 met2::GAL7-lacZ*
L4038[e]	*MAT***a** *leu2Δ2 ura3-52*
L4717[e]	*MAT***a** *ade2 can1-100 his3-11,15 leu2-3,-112 trp1-1 ura3-1*
L4718[e]	*MATα ade2 can1-100 his3-11,15 leu2-3,-1132 trp1-1 ura3-1*
Y388[f]	*MAT***a** *ade2 ade3 ura3 leu2 lys2*
YPN100	*MAT***a** *ade2 can1-100 his3-11,15 leu2-3,-112 trp1-1 ura3-1 nab3-10*
YPN101	*MATα ade2 can1-100 his3-11,15 leu2-3,-1132 trp1-1 ura3-1 nab3-10*
YPN102	*MAT***a** *ade2 can1-100 his3-11,15 leu2-3,-112 trp1-1 ura3-1 nab3-11*
YPN103	*MATα ade2 can1-100 his3-11,15 leu2-3,-1132 trp1-1 ura3-1 nab3-11*
YSW501-1C	*MAT***a** *leu2Δ2 ura3-52 his3 trp1-289 nab3Δ2::LEU2 (*pNAB3.14 [*GAL1::NAB3*])
YSW503	*MAT***a** *leu2Δ2 ura3-52 his3 trp1-289 nab3Δ2::LEU2* (pNAB3.31 [*nab3-3*])
YSW504	*MAT***a** *leu2Δ2 ura3-52 his3 trp1-289 nab3Δ2::LEU2* (pNAB3.33 [*nab3-1*])
YSW506	*MAT***a** *leu2Δ2 ura3-52 his3 trp1-289 nab3Δ2::LEU2* (pNAB3.26 [*nab3-4*])
YSW550-1D	*MATα leu2Δ2 ura3-52 his3 trp1-289 nab3Δ2::LEU2 TRP1::nab3-3*
YSW900	*MATα ade2 ade3 ura3 leu2 lys2 nab3Δ2::LEU2 TRP1::nab3-3* (pNAB3.48 [*ADE3 NAB3*])
YSW901	*MATα ade2 ade3 ura3 leu2 lys2 nab3Δ2::LEU2 TRP1::nab3-9*
YSW911	*MATα ade2 ade3 ura3 leu2 lys2 nab3Δ2::LEU2 TRP1::nab3-9 ctk1Δ1*

[a] Brachmann *et al.* (1998).
[b] Nonet *et al.* (1987).
[c] Yuryev and Corden (1996).
[d] James *et al.* 1996.
[e] Gift of C. A. Styles and G. R. Fink (Whitehead Institute, MIT).
[f] Bender and Pringle (1991).

A *NRD1*-promoter vector, pJC652, was designed to construct the *nrd1-CID*Δ and *nrd1-CID* constructs and for use in generation of temperature-sensitive mutations. This vector is comprised of 1 kb of upstream sequence (up to and including the *NRD1* initiation codon). Adjacent to the initiation codon, an artificial *Sma*I site was engineered, followed by the endogenous 3′ *Eco*RI site and the HA-tag. The vector permits easy in-frame subcloning using *Sma*I/*Eco*RI-digested PCR fragments and provides a convenient restriction site, which was used for gap repair in the generation of temperature-sensitive mutations. Oligos JC835 (5′-GCCGAATTCT GCCCG GGCAT TATGG GATGT TTAGT AT-3′) and JC836 (5′-CGA TAAGCTTG AAAG CCGCT TTA-3′) were used to generate a product that spanned the natural *Hin*dIII site 1 kb upstream of *NRD1* coding sequence to the initiation codon. Immediately downstream of the initiation codon, JC835 contains *Sma*I and *Eco*RI sites. The fragment was cut with *Eco*RI and *Hin*dIII and ligated to a pNRD1-HA *Eco*RI/*Hin*dIII fragment. The resulting clone was transferred to pRS415 via *Xho*I/*Sac*I digestion and ligation.

Domain deletion constructs were designed to test the importance of Nrd1p motifs for viability and were used to map the positions of temperature-sensitive mutations. *Sma*I/*Eco*RI-digested pJC652 was ligated to *Eco*RI/*Sma*I-digested PCR products from JC841 (5′-GGCGAATTC TTGGG ATCCAG TGATA GTTGT-3′) and JC842 (5′-TCCCCCGGG GACGA CGATT TTCAA AA-3′) and JC1111 (5′-AAG CCCGGG CAACT AT CACT GGATCC CAA-3′) and SD2486 (5′-CAGAA ATTAT ATATA GAGGT-3′) to produce pJC583 (*nrd1-CID*) and pJC643 (*nrd1-CID*Δ), respectively. In order to verify that the pJC652-derived N-terminal sequence alterations had no phenotype of their own, an otherwise wild-type construct was generated by ligating *Eco*RI-digested JC1110 (5′-AAGAATTC ACAACT ATCACT GGATCC CAA-3′) and JC1120 (5′-GAGCA

TABLE 2

Plasmids used in this study

Name	Description
pNrd4	Genomic *NRD1 Hin*dIII fragment in pRS426[a]
pNrd1-Not	*NRD1* in pRS426 with *Not*I site engineered at termination codon
pNRD1-HA	pNrd1-Not with HA-tag in *Not*I site
pJC504	pNrd1-Not was transferred to pRS414 and HA-tag was engineered in *Not*I site
pJC580	HA-tagged *NRD1* in pRS415
RP112[b]	6.9-kb *Hin*dIII fragment of *RPB1 (*ARS/CEN,*URA3*)
pYAt[c]	6.9-kb *Hin*dIII fragment of *RPB1* with HA-tag *(*ARS/CEN,*LEU2)*
pY1WT(9)[c]	Derivative of pYAt with 9 repeats of the Rpb1p CTD
pY1WT(10)[c]	Derivative of pYAt with 10 repeats of the Rpb1p CTD
pJC652	*NRD1* promoter vector (see text for details) in pRS415
pJC583	*nrd1-CID* construct (with HA-tag) in pRS415
pJC605	*nrd1-RS*Δ construct (with HA-tag) in pRS415
pJC606	*nrd1-RRM*Δ construct (with HA-tag) in pRS415
pJC643	*nrd1-CID*Δ construct (with HA-tag) in pRS415
pJC951	*nrd1-51* plasmid recovered from temperature-sensitive screen
pJC955	*nrd1-60* plasmid recovered from temperature-sensitive screen
pJC956	*nrd1-83* plasmid recovered from temperature-sensitive screen
pJC719	*nrd1-51* CID mutation subcloned to pJC580-*nrd1-101*
pJC720	*nrd1-60* RRM mutation subcloned to pJC580-*nrd1-102*
pSUP8	*NAB3* genomic fragment (2μ/*URA3*) recovered from high-copy suppression analysis
pNAB3.8	*Nci*I/*Eco*RI fragment from pNAB3.3[d] subcloned into pSP72
pNAB3.14[d]	YCp50 8.0-kb clone containing entire *NAB3* gene
pNAB3.18[d]	*NAB3* gene under control of Gal1 promoter
pNAB3.31	*Xho*I/*Bam*HI fragment of *nab3-3* cloned into pRS316
pNAB3.48[e]	4.5-kb *Xho*I/*Xba*I fragment of *NAB3* cloned into pTSV31A
pNAB3.49	*Xho*I/*Bam*HI fragment of *NAB3* cloned into pRS317
pNAB3.50	*Xho*I/*Bam*HI fragment of *nab3-3* cloned into pRS317

[a] Sikorski and Hieter (1989).
[b] Nonet *et al.* (1987).
[c] West and Corden (1995).
[d] Wilson *et al.* (1994).
[e] Bender and Pringle (1991).

AATAA AGGGT GGAGT-3′)-amplified PCR fragment into *Eco*RI-digested pJC583. No phenotype was observed when this was the sole *NRD1* allele. Deletion of the RRM motif was achieved by PCR amplification of pNRD1-HA with oligos SD2485 (5′-GTACT TTTCTC CAAGC ACGA-3′) and JC1103 (5′-GGACTAGT ATCTGG TGGCAA TGTAG AGT-3′) and SD2486 and JC1102 (5′-GGACTAGT ACTAGG TGGGG AGTTG GTTT-3′). The two products were cut with *Spe*I, ligated overnight at 14°, and reamplified with JC1104 (5′-GAAA CACCT TCACC AACGAT-3′) and SD2485. Products were then cut with *Bst*BI/*Ehe*I and ligated to *Bst*BI/*Ehe*I-cut pJC504. Similarly, deletion of the RE/RS motif used SD2485 and JC1101 (5′-GGACTAGT ACCAT ATTCG GTAAT TGTAT-3′) and SD2486 and JC1100 (5′-GGACTAGT CCTCC GGCACC ATTTT CTCA-3′) in the initial PCR reactions, and *Xcm*I/*Bst*BI in the final step. Finally, pJC605 (*nrd1-RS*Δ) and pJC606 (*nrd1-RRM*Δ) were generated by *Xho*I/*SacI* transfer to pRS415.

Plasmids were recovered from temperature-sensitive strains by standard laboratory procedures (Ausubel *et al.* 1995). Sequenced fragments of temperature-sensitive alleles *nrd1-51* and *nrd1-60* were subcloned to generate *nrd1-101* and *nrd1-102*, respectively; both of these alleles include only one mutation. Plasmids pJC580 (*NRD1-HA*) and pJC951 (*nrd1-51*) were transformed into *dam*$^-$ *dcm*$^-$ *Escherichia coli* strain DM1 (Life Technologies, Gaithersburg, MD) and recovered; nonmethylated plasmids were cut with *Bcl*I/*Xho*I, and 7.9-kb (derived from pJC580) and 1.1-kb (derived from pJC951) products were ligated to generate pJC719. Plasmids pJC504 (*NRD1-HA*) and pJC955 (*nrd1-60*) were cut with *Ehe*I/*Bst*BI; 7.3- and 0.5-kb fragments, respectively, were ligated. The resulting clone was subcloned to pRS415 by *Xho*I/*Sac*I fragment ligation to produce pJC720.

Isolation of *nrd1* temperature-sensitive alleles: Temperature-sensitive alleles of *nrd1* were isolated via PCR mutagenesis and gap repair (Muhlrad *et al.* 1992). Mutagenic PCR was carried out in a 100-μl reaction containing 5 units *Taq* polymerase; 10 mm Tris-HCl (pH 8.3); 50 mm KCl; 1.5 mm $MgCl_2$; 0.2 mm each dATP, dGTP; 1 mm each dCTP, dTTP; 1 μm each JC1120 and JC1121 (5′-CCCCG CTCCTT CCCTT TACGA-3′), and 10 ng pJC504 template. After 10 cycles, $MnCl_2$ was added to 100 μm, and the reaction was carried out for an additional 30 cycles with an annealing temperature of 55°. Reaction products were cotransformed in a 10:1 molar ratio with *Sma*I-digested pJC652 into YJC582. Transformants were selected on CSM-Leu plates, replica plated to CSM-Leu plates containing 0.1% 5-FOA, and then replica plated to CSM-Leu plates at 25° and 37°. Approximately 10^4 colonies were screened, yielding 50 candidates (*nrd1-51* through *nrd1-100*). Six of these candidates (*nrd1-51, nrd1-52, nrd1-53, nrd1-54, nrd1-60,* and *nrd1-83*) were transformed with pNRD1-HA, which complemented the phenotype in all six cases. No other candidates were tested for complementation by pNRD1-HA.

Mapping and sequencing *nrd1* temperature-sensitive mutations: In order to map the location of mutations imparting the temperature-sensitive phenotype, we performed complementation by gap repair. Linearized plasmids were transformed into temperature-sensitive strains and selection was carried out at 37°. Plasmids used were: pJC605 (*Spe*I cut), pJC606 (*Spe*I cut); pJC583 (*Bam*HI cut); and pJC643 (*Sma*I cut). Complementing plasmids showed 500 to >1000 colonies per plate, while noncomplementing plasmids showed two to three orders of magnitude fewer colonies. Using this data, we deduced the approximate domain of the temperature-sensitive mutation and sequenced that region. We subcloned the sequenced areas of *nrd1-51* and *nrd1-60* as outlined in the *Plasmids* section, and we renamed the resulting temperature-sensitive alleles *nrd1-101* and *nrd1-102*, respectively.

Synthetic lethality with CTD truncation mutations: Strains used in CTD synthetic lethality assays were made by transforming YJC546 with a pRS414-derived (Sikorski and Hieter 1989) plasmid encoding the appropriate *NRD1* allele followed by counterselection on 5-FOA. Resulting strains were transformed with pRP112 (Nonet *et al.* 1987) and selected for Ura^+ phenotype with no selection for Leu^+; Ura^+/Leu^- strains carrying *NRD-HA*, *nrd1-51*, and *nrd1-83* were named YJC1111, YJC1115, and YJC1119, respectively. These strains were then transformed with empty vector (CEN/*LEU2*) or plasmids encoding wild-type *RPB1*, or *rpb1* derivatives with CTD truncations to 10 or 9 repeats. Multiple independent transformants were tested for viability on 5-FOA as in the domain deletion analysis. No significant difference was seen in the results if the strains were grown overnight in CSM-Leu or CSM-Ura-Leu prior to 5-FOA selection.

High-copy suppression of *nrd1* temperature-sensitive alleles: A high-copy suppressor screen was performed using a 2μ/*URA3* library (average insert is ~7 kb) generously provided by C. Connelly (Connelly and Hieter 1996). In the first screen, YJC818, a *nrd1-51* strain, was transformed with the library, plated on CSM-Ura, and grown for 24 hr at 25° to allow accumulation of high-copy number. Plates were subsequently transferred to 37° to select for the presence of high-copy suppressors. One plate was left at 25° to determine transformation efficiency. Of $\sim 10^4$ transformants screened, eight colonies grew at 37°, and the appropriate high-copy plasmid was recovered. Multiple restriction digests indicated the presence of three different plasmids, pSUP1, pSUP5, and pSUP8, which were obtained one, four, and three times, respectively. Approximately 500 bp from each end of the insert was sequenced. Similar high-copy screens were performed on *nrd1-53* and *nrd1-60*, but no suppressors were found.

Two-hybrid analysis of *Nrd1p-Nab3p* interactions: The yeast two-hybrid system of James *et al.* (1996), consisting of the efficient selection strain PJ69-4a (harboring selectable *GAL* UAS-dependent *HIS3* and *ADE2* reporter genes) and improved Gal4 activation domain (GAD) and DNA-binding domain (GBD) fusion plasmids, was used to identify Nrd1p interaction partners. GBD-Nrd1p fusions were constructed in the *URA3*-marked plasmids pGBDU-C1 and pGBDU-C3. A *Bam*HI/*Eco*RI fragment of *NRD1* encoding residues 169–560 was excised as a *Bam*HI/*Sal*I fragment from pET21b-Nrd1(169–560) (Steinmetz and Brow 1998) and cloned into *Bam*HI/*Sal*I-digested pGBDU-C3 to generate pGBDU-Nrd1(169–560). To create pGBDU-Nrd1(1–560), a fragment encoding Nrd1p residues 1–169 was generated by PCR of a *NRD1* plasmid with primers Nrd1–5′NdeI (5′-CTAAA CATCC CATATG CAGCA GGACG AC-3′) and Nrd1-Bam169 (5′-GCTTG GGATCC AGTGA TA-3′). The NdeI-digested PCR product was blunted by filling in with Klenow, then digested with *Bam*HI and ligated into *Sma*I/*Bam*HI-digested pGBDU-Nrd1(169–560). pGBDU-Nrd1(169–265) was created by deleting a *Bgl*II fragment bounded by sites in the Nrd1 coding sequence and in the polylinker of pGBDU-Nrd1(169–560). pGBDU-Nrd1(265–560) was created by subcloning a *Bgl*II/*Sal*I fragment from pGBDU-Nrd1(169–560) into pGBDU-C1 to obtain the correct reading frame fusion. pGBDU-Nrd1(169–560RSΔ) was constructed by substituting a *Bam*HI/*Kpn*I fragment from the *nrd1-RS*Δ plasmid, pJC605, into pGBDU-Nrd1(169–560).

The set of yeast two-hybrid libraries constructed by James *et al.* (1996), which have yeast genomic fragments fused to the Gal4 activation domain in all three reading frames in the *LEU2*-marked plasmids pGAD-C1, pGAD-C2, and pGAD-C3, was used to transform strain PJ69-4a harboring pGBDU-Nrd1(1–560). A portion of each transformation reaction was plated onto −Ura −Leu medium to determine the number of transformants, and the remainder was plated on −Ura −Leu −His to select for transformants that received GAD fusions allowing activation of the *HIS3* reporter gene. After growth at 30° for 1 wk under these low-stringency conditions, colonies were replica plated onto −Ura −Leu −Ade medium to select for those transformants that also allow activation of the more stringent *ADE2* reporter. DNA was isolated from colonies appearing 1–5 days after replica plating, and the genomic fragment fused to GAD identified by PCR amplification followed by sequencing with primers GAD5′ (5′-AAGAT ACCCC ACCAA ACCC-3′) and GXD3′ (5′-TTGAG ATGGT GCACG ATGC-3′). Dependence on the GBD-Nrd1 bait for growth on −Ade and −His was verified after selection against pGBDU-Nrd1(1–560) on 5-FOA.

Isolation of *nab3* temperature-sensitive alleles: The *nab3-1*, *nab3-3*, and *nab3-4* mutant alleles were generated by mutagenic PCR using MSS44 (5′-TAATA CGACT CACTA TAGGG AGA-3′) and MSS45 (5′-CATAC GATTT AGGTG ACACT ATAG-3′) and pNAB3.8 (Wilson *et al.* 1994) as described previously (Minvielle-Sebastia *et al.* 1998). The mutagenized DNA and *Sty*I-cut pNAB3.14 were cotransformed into YSW501-1C, and the cells were plated at 24° on SD-Trp. After 3 days, visible colonies were replica plated onto 5-FOA plates and incubated at either 24° or 37°. Colonies that grew at 24° but not 37° were restreaked on SD-Trp. The temperature-sensitive phenotype was confirmed by isolating *nab3* plasmids and recloning of the mutant alleles into pRS314 followed by transformation into YSW501-1C. All mutant alleles were sequenced completely. Several *nab3* mutant strains carried alleles with multiple missense mutations including *nab3-1* (F371I, Q520H), *nab3-3* (I84T, E128D, E129G, F371L, H450R), and *nab3-4* (A312G, L314S, M388V). To confirm that the temperature-sensitive mutation in *nab3-3* was F371L, the *nab3-10* allele was constructed using mutagenic oligonucleotides and subsequently integrated into the *NAB3* chromosomal locus in both L4717 and L4718 strains. Plasmid pNAB3.16 was used as a template for primary PCR reactions using MSS639 (5′-CCCAT CGATTT CTGCA CAGCA ACAAGC-3′) and MSS642 (5′-GCTTT GAGGG TTGTC AAGCT GAATG AATCCA AAGGC-3′) to generate the *nab3-10* 5′ fragment and MSS641 (5′-CATTC AGCTT GACAA CCCTC AAAGC GTTAG AGA TGC-3′) and MSS640 (5′-CCCGG ATCCG CTGTT CTTTA AAGC GCC-3′) for the 3′ fragment (mutations are underlined). For the secondary PCR reaction, primary PCR products were used as the template and MSS639 and MSS640 as primers. The resulting DNA was cut with *Cla*I and *Bam*HI and ligated to *Cla*I/*Bam*HI-digested YIp5. The resulting pNAB3.60 plasmid was linearized with either *Nhe*I or *Hin*dIII and transformed into L4717 and L4718. Following passage on SD-Ura and 5-FOA plates, transformants were tested for growth at 24°, 30°, and 36°. Temperature-sensitive alleles were recovered by gap repair, and the *nab3-10* gene was sequenced completely to confirm the presence of the single F371L missense mutation.

The growth properties of *nab3-3* and *nab3-10* were identical, demonstrating that the single missense mutation was responsible for temperature-sensitive growth.

The *nab3-9* strain was isolated during a synthetic lethal screen. Briefly, Y388 and YSW550-1D were mated, the resulting diploids were dissected, and haploid *ade2 ade3 nab3-3* progeny were identified following transformation with pNAB3.48. Dissected haploids were scored for deletion of *NAB3* (Leu^+), presence of *nab3-3* (Trp^+), and positive sectoring (Sec^+). One of these haploids, YSW900, was plated at a density of 2000 cells/plate and immediately irradiated with UV light in a Stratalinker (Stratagene, La Jolla, CA) to ~10% survival. Following mutagenesis, cells were incubated for 3–5 days at 30° and scored for their ability to sector. The majority of the cells (>95%) remained Sec^+. Nonsectoring (Sec^-) colonies were restreaked twice on YPD and tested for temperature-dependent sectoring. One of these strains, YSW901, was unable to sector at 30° but sectored at 24°. This temperature-dependent sectoring was complemented by either a *NAB3* or *nab3-3* plasmid-borne allele, suggesting that YSW901 carried a new *nab3* temperature-sensitive allele. The mutant allele (*nab3-9*) was recovered by plasmid rescue and was found to contain a new missense mutation in the RRM, P374L, in addition to the five *nab3-3* missense mutations. The *nab3-11* strain, which contains only two missense mutations (F371L and P374L), was constructed essentially as described for *nab3-10*, except that the primary PCR reaction used MSS639 and MSS644 (5′-GCTTT GAGTG TTGTC AAGCT GAATG AATCC AAAGG C-3′) for the 5′ fragment and MSS643 (5′-CATTC AGCTT GACAA CACTC AAAGC GTTAG AGATGC-3′) and MSS640 for the 3′ fragment. The growth characteristics of *nab3-9* and *nab3-11* were identical at 24°, 30°, and 36°.

Extragenic suppression of *nab3-9*: Spontaneous extragenic suppressors were isolated using the *nab3-9* strain, which is growth defective at 30°. Briefly, 5×10^7 YSW901 cells were plated at 30° for 3–4 days. Over 800 Ts^+ colonies were selected, restreaked, and then tested for growth at 24° and 14°. Of the 30 Cs^- colonies recovered, five showed linkage of the Ts^+/Cs^- phenotypes when backcrossed to YSW901. Complementation analysis was performed, and representatives from each group were cloned by complementation of the Cs^- phenotype using a YCp50 yeast genomic library.

Immunoprecipitation analysis: Monoclonal antibody 12CA5 was coupled to protein A/G beads (Pierce, Rockford, IL). A total of 60 μl of beads was bound per 10 ml of 12CA5 culture supernatant and crosslinked to dimethylpimelimidate essentially as described (Harlow and Lane 1988). Coupled beads (40 μl) were incubated with 1.25 mg of yeast whole cell extract in 1 mg/ml BSA, 50 mm Tris-HCl (pH 7.6), 0.05% NP-40, 2 mm $MgCl_2$, 100 mm NaCl with protease (1 mm phenylmethylsulfonyl fluoride, 2 mm pepstatin, 0.6 mm leupeptin, 2 mm benzamidine HCl) and phosphatase (0.2 mm Na_3VO_4, 50 mm KF, 15 mm β-glycerolphosphate) inhibitors in a reaction volume of 2 ml for 2 hr at 4° in the presence or absence of 100 ng/μl RNase A. Beads were then washed batch-wise five times in 500 μl binding buffer (without BSA). Elution was carried out by boiling for 3 min in 60 μl 2× Laemmli buffer without β-mercaptoethanol.

Preparation of extracts and Western blot analysis: Yeast total protein extracts were prepared essentially as described (Patturajan *et al.* 1998a). Cell pellets were resuspended in an approximately equal volume of buffer A (200 mm Tris-HCl, pH 8.0, 320 mm ammonium sulfate, 5 mm $MgCl_2$, 10 mm EGTA, 20 mm EDTA, 1 mm dithiothreitol, 20% glycerol) with protease inhibitors and phosphatase inhibitors. Acid-washed 425-660 micron beads (Sigma, St. Louis) were added up to the meniscus and vortexed 10 times for 20 sec each with intervals of 30 sec on ice. The lysate was cleared by centrifugation at 10,000 × *g* for 10 min. Western blot analysis was performed with tissue culture supernatant of mAb 12CA5 (Wilson *et al.* 1984) diluted 1:10 in 1× PBS with 0.05% Tween-20, 5.0% dried milk.

Dephosphorylation of yeast protein extracts: Yeast total protein extract (~100 μg) was diluted 10-fold and dialyzed twice for 1.5 hr each against 5×10^3 volumes of λ phosphatase buffer (50 mm Tris-HCl, pH 7.5, 0.1 mm EDTA, 5 mm DTT, 0.01% Brij 35, 10% glycerol). Each extract was divided in half, brought to 2 mm $MnCl_2$, and incubated in the presence or absence of 400 units of λ phosphatase (New England Biolabs, Beverly, MA) for 1 hr at 30°.

RESULTS

Identification of essential Nrd1p domains: Sequence analysis reveals three conserved sequence domains in Nrd1p (Steinmetz and Brow 1996). The N terminus of the protein contains similarity to the CID of pol II CTD-binding proteins called SCAFs (Patturajan *et al.* 1998b), and has been shown to bind to the CTD by yeast two-hybrid analysis (Yuryev *et al.* 1996). Also evident are an RRM and a 21-amino acid RE/RS domain, rich in alternating arginine and glutamate or serine dipeptides. To determine which of these domains is necessary for the essential function of Nrd1p, we deleted each one and tested for viability by plasmid shuffle. Strain YJC582 (*nrd1Δ*, *NRD1-HA* on a 2μ/*URA3* plasmid) was transformed with domain deletion constructs and counterselected on 5-FOA at multiple temperatures (15°, 20°, 25°, 30°, and 37°). Expression of the truncated proteins was verified by Western blot (data not shown).

The results of this analysis are summarized in Figure 1. Deletion of the RRM does not support viability, a result consistent with an essential role for RNA binding (Steinmetz and Brow 1998) by Nrd1p *in vivo*. The only other lethal deletion removes all sequences C-terminal to the CID, including the RRM.

As previously observed, deletion of the CID is not

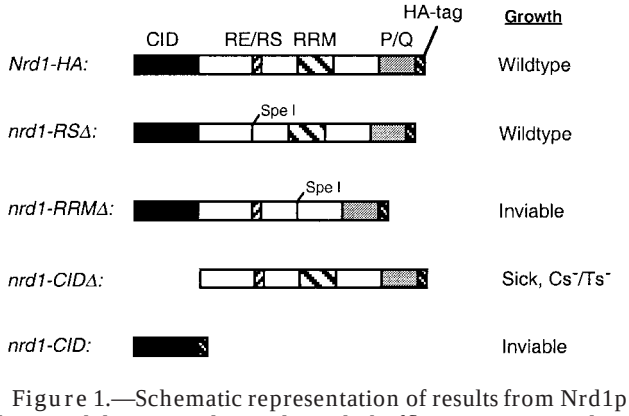

Figure 1.—Schematic representation of results from Nrd1p domain-deletion analysis. Plasmid shuffle assay was used to examine the viability of yeast strains carrying the indicated domain deletion. Domains include the N-terminal CID, a motif rich in arginine/glutamate and arginine/serine dipeptides (RE/RS), an RRM, a C-terminal region rich in proline and glutamine (P/Q), and an HA-tag.

lethal (Steinmetz and Brow 1998). However, we observed that deletion of this domain confers partial cold- and temperature-sensitive phenotypes as well as an increase in doubling time. Colonies grown on rich or minimal plates are heterogeneous in size, and the proportion of cells that are viable upon counterselection of the wild-type allele is much lower than that of other viable alleles. The *nrd1Δ39-169* allele (Steinmetz and Brow 1998) did not show these phenotypes, suggesting that the amino terminal 38 residues may provide partial CID function. The importance of the first 38 amino acid residues is supported by the isolation of a temperature-sensitive mutation in this region (see below). Since *nrd1Δ39-169* is not HA-tagged, it remains possible that the HA-tag present on the *nrd1-CIDΔ* allele compromises Nrd1p function. However, we feel that this is unlikely because the HA-tagged wild-type allele shows no abnormal growth phenotype.

The RE/RS domain is expendable for normal growth. However, while indirect immunofluorescence shows wild-type Nrd1p is nuclear at steady state, deletion of the RE/RS motif leads to increased Nrd1p levels in the cytoplasm (data not shown). Interestingly, similar "leaky" nuclear localization has been observed upon deletion of the RS domains of mammalian SF2/ASF, SRp40, SC35, and SRp20 (Caceres *et al.* 1998).

Temperature-sensitive alleles of *nrd1*: Previously, a temperature-sensitive missense mutation was isolated in the Nrd1p RRM, V368G (Steinmetz and Brow 1996). To allow further characterization of functional domains in Nrd1p, additional temperature-sensitive alleles of *nrd1* were isolated using PCR mutagenesis and gap repair (Muhlrad *et al.* 1992). Approximately 10^4 transformants were screened, and 50 candidate strains were isolated based on their inability to grow at 37°. Of these strains, 6 were tested for complementation by pNRD1-HA, and all 6 strains were shown to carry recessive temperature-sensitive *nrd1* alleles (*nrd1-51*, *nrd1-52*, *nrd1-53*, *nrd1-54*, *nrd1-60*, and *nrd1-83*, data not shown). For 4 of these alleles, *nrd1-51*, *nrd1-54*, *nrd1-60*, and *nrd1-83*, the regions with mutations responsible for the temperature-sensitive phenotype were deduced by gap repair with linearized domain deletion constructs as described in materials and methods. Alleles *nrd1-51* and *nrd1-54* were complemented by the linearized *nrd1-CID* construct, as well as *nrd1-RSΔ* and *nrd1-RRMΔ*, but not by the linearized *nrd1-CIDΔ* construct, suggesting that these alleles contain mutations in the CID. Similarly, temperature sensitivity of *nrd1-60* and *nrd1-83* was complemented by every construct tested except for *Spe*I-digested *nrd1-RRMΔ* construct, suggesting that RRM mutations confer temperature sensitivity in these alleles. To verify the presence of mutations at the indicated domains, the appropriate domain was sequenced (Figure 2A).

To establish whether the conditional phenotypes of *nrd1-51* and *nrd1-60* are due to the identified mutations, the sequenced portions of these alleles were subcloned into an otherwise normal *NRD1-HA* plasmid. The resulting alleles were named *nrd1-101* (S16P) and *nrd1-102* (V379G), respectively. These particular mutant alleles were chosen because serine 16 is conserved between Nrd1p and SCAF8, and valine 379 is in the predicted ribonucleoprotein (RNP1) motif of the RRM. While there was no phenotypic difference observed between *nrd1-60* and *nrd1-102*, *nrd1-101* was more leaky at 37° than *nrd1-51* and showed even less temperature sensitivity when plated on galactose plates (Figures 2B and 4B, and data not shown). The presence of multiple mutations in *nrd1-51* is indicated by these observations.

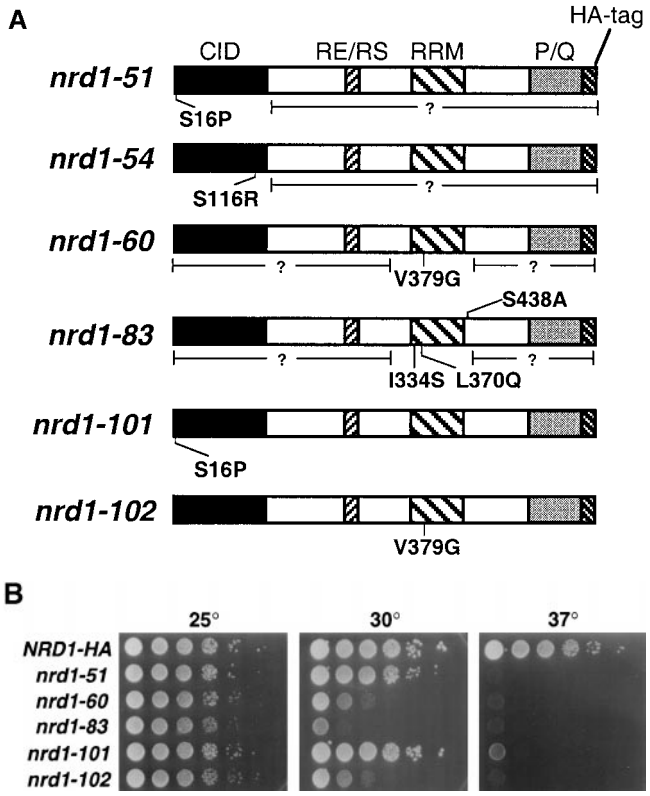

Figure 2.—Temperature-sensitive alleles of *nrd1* used in this study. (A) Schematic representation of *nrd1* temperature-sensitive alleles. Regions outlined with a question mark were not sequenced. Mutations in the CID of *nrd1-51* and in the RRM of *nrd1-60* were subcloned to otherwise wild-type *NRD1-HA* to generate *nrd1-101* and *nrd1-102*, respectively. (B) Wild-type and temperature-sensitive strains were grown to saturation, diluted approximately twofold to equal OD_{600}, diluted serially (eightfold), and grown for 48 hr on YPD at indicated temperatures. Growth of strain harboring the *nrd1-54* is similar to that of *nrd1-101* (data not shown).

Temperature-sensitive alleles of *nrd1* are synthetic lethal with truncations of the CTD: Because Nrd1p is similar to the mammalian SCAF8 family of CTD-binding proteins and has a similar organization of domains, we examined potential genetic interactions between *NRD1* and the pol II CTD. Strains YJC1111 (*NRD1-HA*), YJC1115 (*nrd1-51*), and YJC1119 (*nrd1-83*) are congenic and have chromosomal disruptions of the *RPB1* and

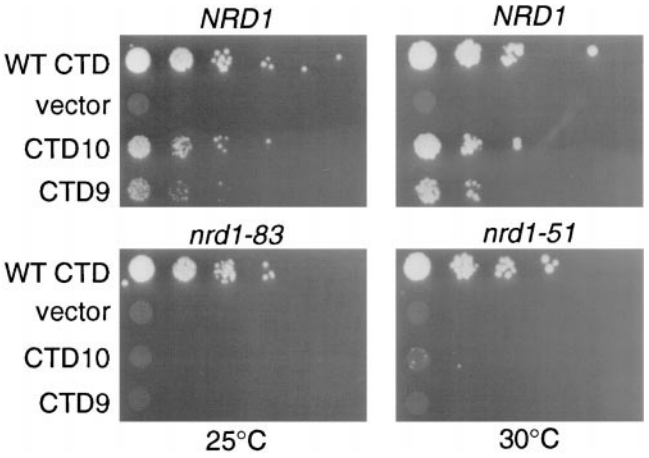

Figure 3.—Synthetic lethality between *nrd1* temperature-sensitive mutations and CTD truncations. Strains YJC1111 (*NRD1-HA*, top), YJC1115 (*nrd1-51*, bottom right), and YJC1119 (*nrd1-83*, bottom left) were transformed with vector alone or versions of *RPB1* with 26 (WT CTD), 10 (CTD10), or 9 (CTD9) repeats of the CTD heptad consensus sequence on a *LEU2*-marked plasmid. Transformants were grown to saturation in CSM-Leu-Ura media, diluted serially (eightfold), and plated onto 5-FOA plates at the indicated temperatures. Strain YJC1119 was plated at 25° because *nrd1-83* strains grow poorly at 30°.

NRD1 loci that are covered with plasmids carrying wild-type *RPB1* (CEN/*URA3*) and the indicated *nrd1* (CEN/*TRP1*) allele. Each of these strains was transformed with vector alone or derivatives of *RPB1* with 26 (wild-type), 10, or 9 repeats of the CTD heptad consensus sequence on a *LEU2*-marked CEN plasmid (West and Corden 1995). Transformants were serially diluted and plated onto CSM-Leu 5-FOA plates to counterselect the wild-type *RPB1* allele. Most combinations of CTD truncation with *nrd1* temperature-sensitive alleles do not support viability (Figure 3), demonstrating a synthetically lethal phenotype. A small percentage of cells survive in the *nrd1-51*/CTD10 strains. These may be revertants caused by CTD expansion as observed previously (West and Corden 1995). Alternatively, some combination of copy numbers of the plasmid-borne CTD10 and *nrd1-51* alleles may suppress the synthetically lethal phenotype allowing growth of these cells.

***NAB3* is an allele-specific high-copy suppressor of *nrd1-51*:** A high-copy suppressor screen of *nrd1-51* was performed using a 2μ/*URA3* genomic library with an average insert size of 7 kb (Connelly and Hieter 1996). Eight suppressor strains were isolated and high-copy plasmids were recovered. One strain contained a *NRD1* plasmid, and the remaining seven had one of two different plasmids (pSUP5 or pSUP8). Partial sequences indicated that both of these plasmids carry a copy of *NAB3*, a yeast hnRNP gene (Wilson *et al.* 1994). To verify that Nab3p overexpression suppressed the *nrd1-51* allele, YJC818 was transformed with vector alone or pNAB3.18, which has the *NAB3* gene under the control of the GAL1 promoter. As expected, pNAB3.18 suppressed the *nrd1-51* temperature-sensitive phenotype on galactose plates, but not on glucose plates (Figure 4A).

Since *nrd1-51* most likely contains mutation(s) other than S16P, we wanted to verify that Nab3p overexpression suppresses the S16P mutation. However, we could not achieve this using pNAB3.18 because the *nrd1-101* allele is leaky on galactose media. Therefore, we used pSUP8 to examine suppression of *nrd1-101*. Yeast strains carrying the wild-type, *nrd1-51*, or *nrd1-101* alleles were transformed with either empty vector or pSUP8. The growth of the pSUP8-transformed *nrd1-101* strain was indistinguishable from wild type at 37° (Figure 4B). Interestingly, pSUP8 also suppressed the temperature-sensitive phenotype of *nrd1-54*, which, like *nrd1-101*, has a mutation that alters a serine residue (S116R) in the CID and is leaky on galactose (data not shown). Alleles with mutations mapping outside the CID were not suppressed by Nab3p overexpression (*nrd1-60*, *nrd1-83*, and *nrd1-102*; data not shown). The allele specificity of Nab3p overexpression is consistent with a model in which the CID of Nrd1p has a function that is distinct from the rest of the protein and is linked to the yeast hnRNP, Nab3p. Further high-copy screens were performed on *nrd1-53* and *nrd1-60*, but no high-copy suppressors were found (*NRD1* was recovered 10 and 4 times, respectively).

Two-hybrid interactions between Nrd1p and Nab3p: A yeast two-hybrid screen was conducted to identify proteins that interact with Nrd1p *in vivo*, using the improved reporter strain and libraries of James *et al.* (1996). A "bait" construct encoding the first 560 residues of Nrd1p fused to the GBD was used to select Nrd1p interaction partners from a library of yeast genomic fragments expressed as fusions to the GAD. From $\sim 10^6$ transformants subjected to this selection, 13 that showed Nrd1p bait-dependent growth on −his and −ade were analyzed. Two transformants exhibiting robust growth on −his and −ade media were found to contain in-frame GAD fusions to residues 99-766 of Nab3p or to the entirety of Nab3p C-terminal to residue 35, respectively. None of the other 11 positive clones contains an in-frame fusion.

A series of bait fusions expressing different fragments of Nrd1p was used to show that the region between residues 169 and 265 containing the RE/RS domain (residues 245–265) is necessary and sufficient for productive two-hybrid interactions with the GAD-Nab3 fusion (Figure 5). The RE/RS sequence itself, however, is not required for interaction with Nab3p, since the deletion of this sequence from the GBD-Nrd1p(1–560) fusion still allows for productive two-hybrid interactions with GAD-Nab3p. These results define a new functional domain of Nrd1p: a Nab3p-interaction domain located between residues 169 and 244 and situated between the CID and RE/RS domains.

Nrd1p and Nab3p co-immunoprecipitate: To further

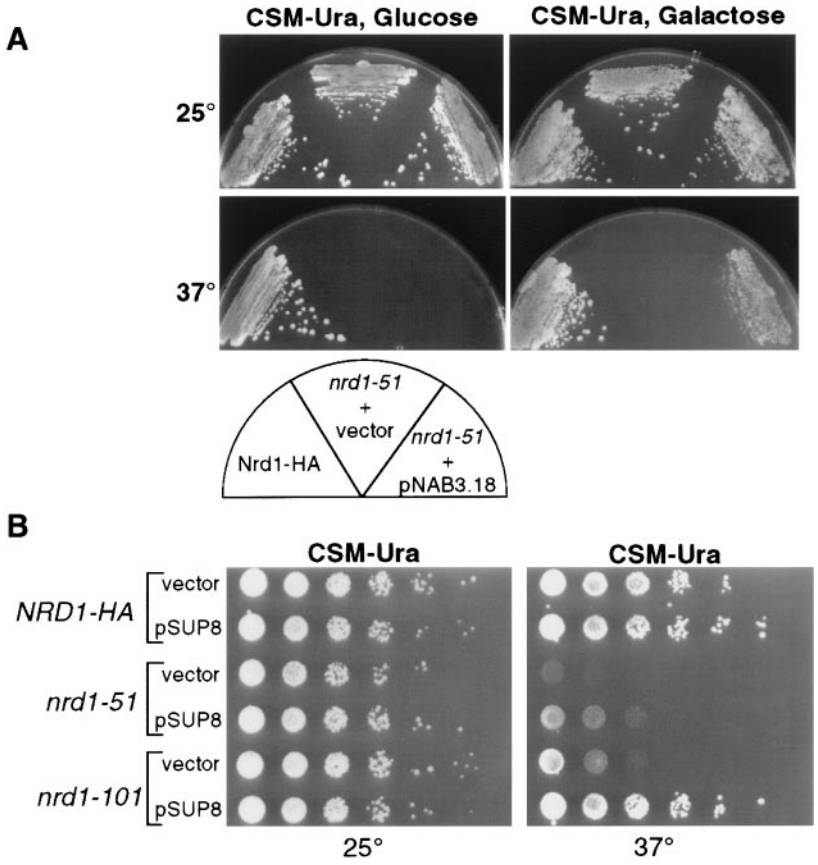

Figure 4.—Nab3p overexpression suppresses *nrd1-51* and *nrd1-101*. (A) Strains YJC582 (Nrd1-HA, 2μ/*URA3*) and YJC818 (*nrd1-51*) transformed with vector alone or pNAB3.18, were grown to saturation, diluted 10-fold, and streaked onto CSM-Ura plates with either glucose or galactose. (B) Strains YJC610 (*NRD1-HA*), YJC818 (*nrd1-51*), or YJC1103 (*nrd1-101*) were transformed with vector alone or pSUP8, a 2μ *URA3*-marked plasmid with a *NAB3* genomic fragment. Transformants were grown to saturation in CSM-Ura media, diluted serially (8-fold), and plated onto CSM-Ura. Plates were incubated for 48 hr at 25 or 37° as indicated.

characterize the *in vivo* Nrd1p and Nab3p interaction, we performed coimmunoprecipitation experiments. Extracts were made from strains YJC610 (*NRD1-HA*) and YJC976 (*NRD1*) and were immunoprecipitated with the anti-HA mAb 12CA5 in the presence or absence of RNase. Proteins in the immunocomplex were separated by gel electrophoresis, were Western blotted, and were probed for the presence of Nab3p with the mAb 2F12 (Figure 6). A small fraction of the Nab3p is immunoprecipitated specifically and in an RNA-independent fashion with Nrd1-HAp.

Characterization of *nab3* mutants: To further examine the role of Nab3p *in vivo*, we generated several temperature-sensitive *nab3* strains. The resulting *nab3-1*, *nab3-3*, and *nab3-4* alleles were sequenced completely and were shown to contain multiple missense mutations (Figure 7A). While the growth properties of these *nab3* strains were similar to a wild-type strain between 14° and 30°, *nab3-1* was growth restricted at 36°, while *nab3-3* and *nab3-4* were inhibited at 37°. Comparison of the missense mutations in these *nab3* strains suggested that RRM mutations conferred temperature sensitivity. This was confirmed in the case of *nab3-3* since the growth characteristics of the *nab3-10* strain, which has a single RRM mutation (Figure 7A), and *nab3-3* are similar at all temperatures tested. The *nab3-9* mutant, which was isolated during a *nab3-3* synthetic lethal screen (see materials and methods), contains an additional RRM mutation (P374L) and was inhibited for growth at 36° (Figure 7). The two RRM mutations (F371L and P374L) are also sufficient to confer temperature sensitivity since the growth properties of *nab3-11*, which contains only the two RRM mutations, and *nab3-9* are similar.

Extragenic suppression of *nab3-9* by *CTK1* kinase domain mutation: To elucidate the essential function of Nab3p, we isolated extragenic suppressors of *nab3-9*. Over 800 colonies that grew at 30° in 3–4 days were selected, restreaked, and tested for cold sensitivity at 14°. Of the 30 cold-sensitive strains that were identified by this analysis, only 5 were able to produce viable spores for cosegregation analysis, falling into two **s**uppressor of ***nab3-3*** (*snb3*) complementation groups. A representative from each group was used for complementation of the cold-sensitive phenotype using a YCp50 genomic library, and the complementing plasmids were recovered and sequenced. The *snb32-1* strain was complemented by an 8-kb chromosome XI fragment which encodes *MRP8*, *SDH3*, *TGL1*, and *CTK1*. Subclones containing individual genes were tested for *snb32-1* complementation. Only *CTK1*, encoding the RNA pol II *c*arboxyl-*t*erminal repeat domain *k*inase (Lee and Greenleaf 1991), was able to restore growth at 14°. To confirm that *CTK1* was allelic to *snb32-1*, *CTK1* was integrated at the *ctk1* locus in the *snb32-1* strain, and the resulting transformant was mated to a *nab3-9* strain. Sporulation and dissection of the resulting diploid did not yield cold-

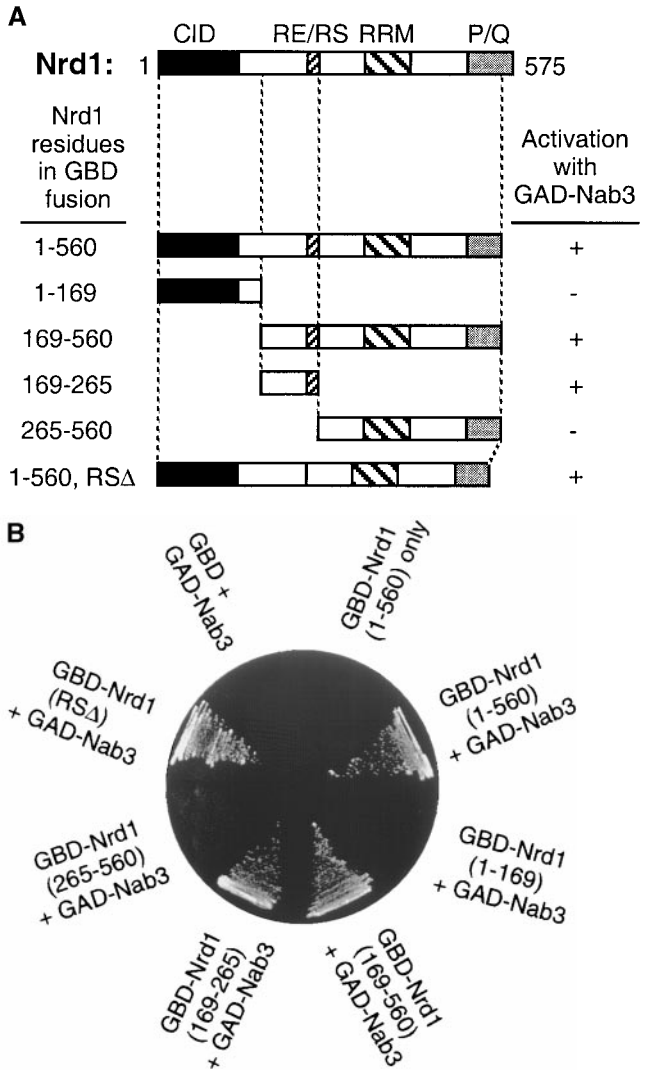

Figure 5.—Two-hybrid interactions between Nrd1p and Nab3p. (A) Schematic illustration of Nrd1p fragments fused to GBD and tested for interactions with Nab3p fused to GAD. Growth on −His and −Ade plates is indicated by +, while − indicates no growth on either −his or −ade. (B) Plate showing growth of PJ69-4a expressing the indicated combinations of GBD-Nrd1p and GAD-Nab3 fusions on −ade medium. The GAD-Nab3p fusion in each case includes residues 99–766 of Nab3p.

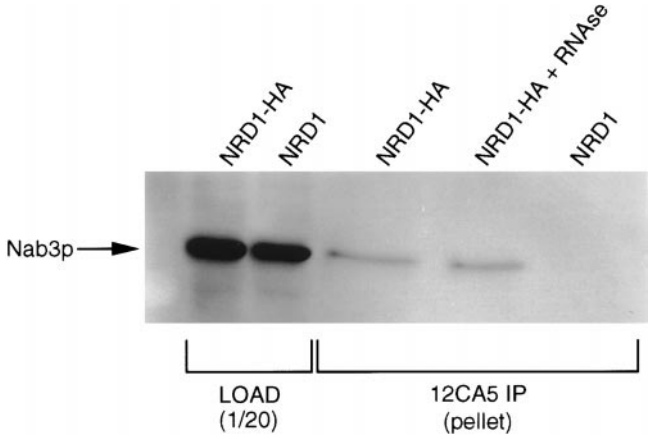

Figure 6.—Nab3p coimmunoprecipitates with Nrd1p. Immunoprecipitation with mAb 12CA5 (anti-HA) was performed using extracts generated from log phase (OD_{600} = 1.0) cells expressing Nrd1p with or without the HA-tag, as indicated. The entire pellet and 5% of the load was run on a 7.5% SDS-PAGE and Western blotted using mAb 2F12 (anti-Nab3) as a probe.

sensitive progeny. In addition, the *ctk1* mutant allele was recovered by gap repair and sequenced. A single missense mutation was discovered within the conserved kinase domain (K211E), suggesting that loss of Ctk1p kinase activity was responsible for *nab3-9* suppression. Consistent with this possibility, disruption of the *CTK1* gene (*ctk1*Δ) in the *nab3-9* strain YSW911 suppressed the temperature-sensitive defect (Figure 7B). Similar analysis showed that the remaining complementation group (*snb31)* was allelic to the adenylate cyclase gene *CYR1*.

Since 25 of the 30 cold-sensitive strains did not produce viable spores for segregation analysis, these suppressor strains were mated to YSW901, and the diploids were plated at 30° to determine if suppression was dominant or recessive. This analysis indicated that 14 of these strains were recessive for suppression, and these cells were transformed with the YCp50 genomic library to identify genes that complement the cold-sensitive phenotype. Of the 14 recessive suppressor strains, 7 showed plasmid linkage for growth at 14° and loss of growth at 30°. Further analysis of these plasmids demonstrated that the gene responsible for suppression was *CTK1*. Therefore, out of 12 suppressor alleles identified, 8 encoded *ctk1* mutant alleles. Subsequent analysis of *NAB3*, *nab3-9*, or *ctk1*Δ/*nab3-9* cells failed to detect significant differences in the expression levels or phosphorylation status of Nab3p (data not shown).

The phosphorylation state of *nrd1-51* is changed by Nab3p overexpression: Nrd1p migrates as multiple bands in Western blot analysis (Steinmetz and Brow 1998; and Figure 8). To test whether the different bands represent phosphoisomers of Nrd1p, we treated whole cell extracts with λ phosphatase and analyzed the resulting treated (or mock-treated) extracts by Western blotting with the HA-tag specific mAb 12CA5. Phosphatase treatment of the extracts revealed the presence of a third, faster migrating band on SDS-PAGE (Figure 8A, lanes 1 and 2), suggesting that, *in vivo*, Nrd1p exists in two different phosphoisoforms.

The consistent presence of both phosphoisoforms of Nrd1p from cells harvested during log phase implies a potential role for phosphorylation in the regulation of Nrd1p. Strengthening that idea, we noted that upon overexpression of Nab3p in the *nrd1-51* strain, YJC818, only the top band is observed (Figure 8B). Similar results are seen with wild-type Nrd1-HAp (data not shown). Since treatment with λ phosphatase results in

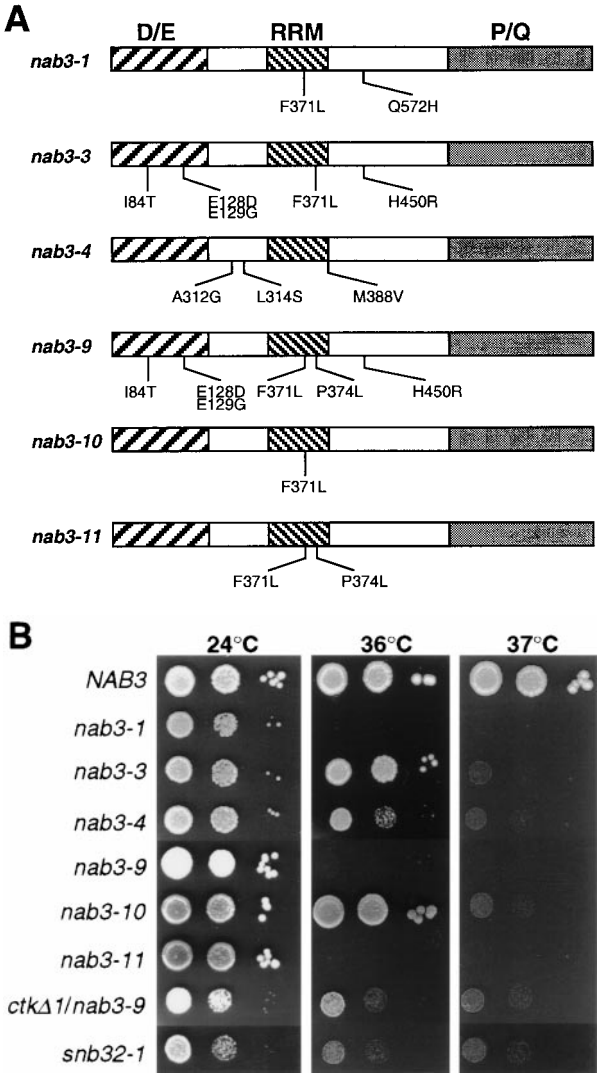

Figure 7.—*nab3* temperature-sensitive alleles. (A) Schematic representation of *nab3* temperature-sensitive alleles. Nab3p structural motifs include the amino terminal region rich in aspartic and glutamic acid residues (D/E), the RRM, and the carboxyl-terminal region rich in proline and glutamine residues (P/Q). All *nab3* mutant alleles were completely sequenced, and the missense mutations in each allele are indicated. (B) Spot plate growth analysis of *nab3*, and *nab3-9* suppressor, strains at 24°, 36°, and 37°.

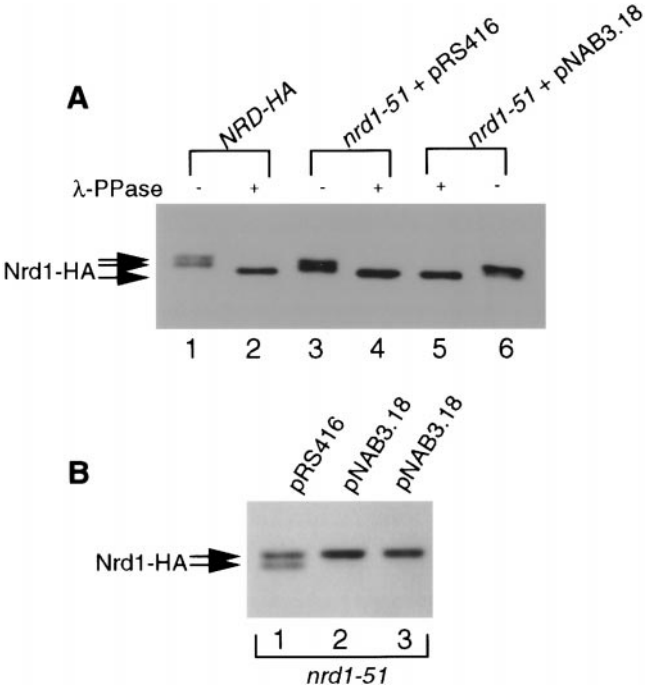

Figure 8.—The phosphorylation state of Nrd1p is altered in response to Nab3p overexpression. (A) Total protein extracts were prepared from YJC610 grown in YPD and YJC818 (transformed with either vector alone or pNAB3.18) grown in CSM-Ura galactose media. Extracts were treated with λ phosphatase (+) or mock-treated (−) as indicated and run on a 10% SDS-PAGE. (B) YJC818-derived extracts described in A are shown on a 7.5% SDS-PAGE. Two independent transformants for pNAB3.18-transformed strains are shown. Extracts shown in lanes 1 and 2 were used for λ phosphatase reactions shown in lanes 3–6 of A. Western analysis was performed using mAb 12CA5.

a band that migrates indistinguishably from the phosphatase-treated wild-type or vector-transformed YJC818 (Figure 8A, lanes 3 through 6), the change in migration is likely due to a change in phosphorylation. Deletion of *CTK1* does not change the migration pattern of Nrd1p on SDS-PAGE (data not shown).

DISCUSSION

The steady-state level of a given mRNA is determined by the relative rates of synthesis and degradation. Synthesis is a multistep process that involves transcription and processing, followed by export of mature RNA from the nucleus. Evidence has been mounting to support a model in which these steps are coupled *in vivo*. hnRNPs are likely to play roles in many of these processes (Siomi and Dreyfuss 1997; Krecic and Swanson 1999). In yeast, for example, Nab4p/Hrp1p has been shown to be involved in 3′ processing both *in vitro* and *in vivo* (Kessler *et al.* 1997; Minvielle-Sebastia *et al.* 1998). Npl3p/Nab1p is genetically linked to 3′ processing factors Rna15p and Nab4p/Hrp1p and is involved in RNA export from the nucleus (Henry *et al.* 1996; Lee *et al.* 1996). The functions of other yeast hnRNPs remain to be elucidated.

Yeast *NRD1* was first cloned based on its ability to downregulate the level of pre-mRNA transcribed from an artificial, intron-containing gene (Steinmetz and Brow 1996). While the data are inconclusive as to whether the decrease in steady-state pre-mRNA is due to a decrease in RNA synthesis or an increase in degradation, the observation of 3′ truncated products suggests that Nrd1p could be involved in premature transcriptional termination, inefficient transcriptional elongation, or degradation via a 3′ to 5′ exonuclease activity (Steinmetz 1997). The genetic interactions presented

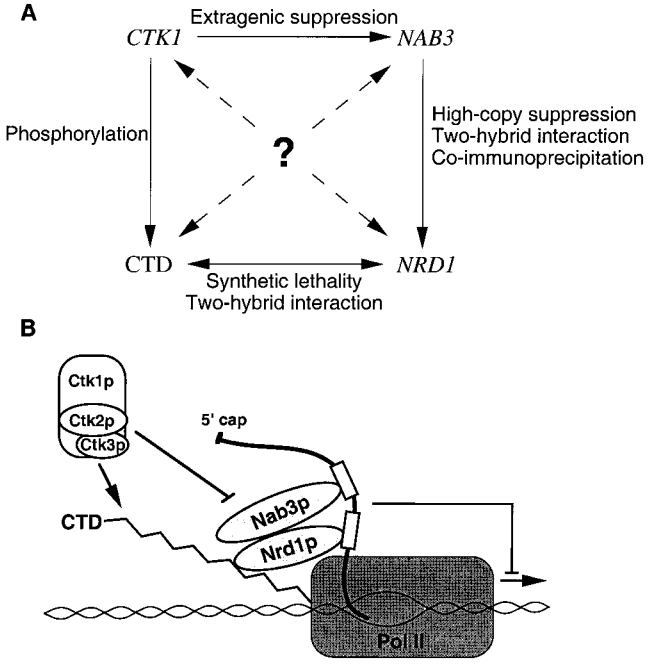

Figure 9.—(A) Schematic overview of the interactions described in this article and elsewhere. (B) A model for Nrd1p-Nab3p function. See text for details.

in this article support a model in which Nrd1p acts at the interface of transcription and processing without ruling out a potential role in degradation. A summary of known interactions, genetic and biochemical, is outlined in Figure 9A.

***NRD1*-CTD interaction:** The similarity of Nrd1p to mammalian SCAF8 suggested initially that Nrd1p could interact with the CTD. This hypothesis has been supported by additional two-hybrid data. First, the Nrd1p CID was shown to interact with the mouse CTD (Yuryev *et al.* 1996). Second, in a genome-wide two-hybrid screen similar to the one described here, a yeast Nrd1p-interacting clone was isolated that encodes the Gal4 activation domain fused to the C terminus of Rpb1p. The clone includes the entire CTD as well as ~120 amino acids N-terminal to the CTD (N. K. Conrad and J. L. Corden, unpublished observations).

We have also used a genetic approach to demonstrate an interaction between Nrd1 and the CTD. Previous studies showed that many of the yeast CTD heptapeptide repeats can be deleted without phenotypic consequences (Nonet *et al.* 1987; West and Corden 1995). Reducing the CTD length to 8–11 repeats yields cold- and temperature-sensitive growth phenotypes (Nonet *et al.* 1987; West and Corden 1995) and results in altered expression of a subset of genes (Scafe *et al.* 1990; Meisels *et al.* 1995). In the current study, we show that truncation of the CTD to 9 or 10 repeats is synthetically lethal with two different temperature-sensitive alleles of *nrd1*. This result is consistent with previous two-hybrid and direct binding experiments with SCAF8. Together they indicate that Nrd1p and pol II function in the same pathway *in vivo*, most likely through direct interaction.

***NRD1-NAB3* interaction:** We have also demonstrated genetic and physical interactions between RNA-binding proteins Nrd1p and Nab3p. Similarities in sequence organization suggest that Nrd1p and Nab3p may play related roles in mRNA biogenesis. Both genes are essential and encode RNA-binding proteins with a single RRM and a carboxyl-terminal proline/glutamine-rich region (Wilson *et al.* 1994; Steinmetz and Brow 1996). Nrd1p and Nab3p differ in that Nrd1p has RE/RS and CTD-interacting domains N-terminal to the RRM, while the corresponding region of Nab3p is highly acidic. Nrd1p is most closely related to mammalian SCAF8 (Corden and Patturajan 1997), while Nab3p is most closely related to the hnRNP C family of mammalian RNA-binding proteins (Wilson *et al.* 1994).

Three lines of evidence suggest a direct interaction between Nrd1p and Nab3p *in vivo*. First, *NAB3* is an allele-specific high-copy suppressor of the *nrd1* CID mutations. Second, Nrd1p and Nab3p interact in a yeast two-hybrid assay. Third, Nrd1p and Nab3p coimmunoprecipitate. The interaction is not mediated by RNA since the two-hybrid interaction is independent of the Nrd1p RRM and extensive RNase treatment did not affect coimmunoprecipitation. The observation that only a fraction of the Nab3p coimmunoprecipitated with Nrd1p may indicate that the interaction is transient or is important for only a small subset of transcripts that contain both Nrd1p- and Nab3p-binding *cis*-elements. Of course, experimental conditions may also affect the efficiency of coimmunoprecipitation. For example, the proteins may dissociate upon lysis or antibody binding may destabilize the interaction. Unfortunately, the coimmunoprecipitation of Nrd1p with anti-Nab3p mAb is technically not feasible because only a small amount of Nab3p immunoprecipitated with mAb 2F12.

Both Nrd1p and Nab3p are hnRNPs that have been shown to play a role in mRNA accumulation. Nrd1p is thought to act early in transcription to mediate the downregulation of transcripts containing negative *cis*-elements (Steinmetz and Brow 1996, 1998; Steinmetz 1997). Nab3p overexpression has been shown to reduce the steady-state level of *CLN3* mRNA (Sugimoto *et al.* 1995). In addition, Nab3p has been implicated in the processing of several intron-containing pre-mRNAs including *CYH2* and *ACT1* (Wilson *et al.* 1994). However, neither *nrd1* nor *nab3* temperature-sensitive strains show an increase in the ratio of unspliced to spliced *ACT1* or *CYH2* RNAs upon shift to the nonpermissive temperature (data not shown). Both Nrd1p and Nab3p could act at the level of transcription elongation and/or termination. Alternatively, these proteins may be involved in turnover of nuclear pre-mRNA.

The synthetic lethality of *nrd1* temperature-sensitive alleles with CTD-truncation mutations indicates that interaction of Nrd1p with the CTD serves an important

function, yet the Nrd1p CID is dispensible for viability. The CID may provide only one of multiple redundant mechanisms to ensure interactions between Nrd1p and pol II. The allele-specific high-copy suppression of temperature-sensitive *nrd1* CID mutant alleles by *NAB3* suggests that Nab3p may provide another mechanism to facilitate Nrd1p-CTD interactions. If Nrd1p interacts with Nab3p and the CTD simultaneously, Nab3p may be in close proximity to the CTD and stabilize the Nrd1p-CTD interactions. This would also provide a framework within which to understand the genetic interactions between *CTK1* and *NAB3* reported here.

Interactions between *CTK1*, *NRD1*, and *NAB3*: Protein phosphorylation is a common thread among the interactions we describe in this article. The pol II CTD, Nrd1p, and Nab3p are all phosphorylated *in vivo* (Dahmus 1996; Figure 8, and data not shown). The identification of a CTD kinase as a suppressor of *nab3-9* provides an additional link from *NAB3* to the CTD (Figure 9A). Precisely how phosphorylation may regulate the function of the CTD, Nrd1p, and Nab3p is not known, but several clues are evident in the results presented here.

CTDK-I is a protein kinase identified initially by its ability to phosphorylate the CTD of pol II *in vitro* (Lee and Greenleaf 1989). This CTD kinase is comprised of three subunits, a cdc2-related catalytic subunit (Ctk1p), a cyclin-related subunit (Ctk2p), and a third subunit of unknown function (Ctk3p) (Lee and Greenleaf 1991; Sterner *et al.* 1995). Deletion of any of the CTDK-I subunit genes is not lethal, but the null mutants display slow growth and cold-sensitive phenotypes (Sterner *et al.* 1995). CTDK-I is not a part of the pol II holoenzyme (Myer and Young 1998), but rather is thought to phosphorylate the newly initiated pol II. Furthermore, CTDK-I stimulates transcript elongation in Hela nuclear extracts (Lee and Greenleaf 1997).

The genetic evidence presented here indicates that CTDK-I may play a role in negatively regulating the functions of Nrd1p and Nab3p. Deletion of *CTK1* suppresses the temperature-sensitive phenotype of *nab3-9*. Furthermore, overexpression of Nab3p severely inhibits the growth of a *ctk1*Δ strain, and *nrd1-102* is a weak suppressor of the cold-sensitive phenotype of *ctk1*Δ (data not shown). All of these results are consistent with opposing effects of Ctk1p and Nrd1p-Nab3p. Whether the interactions between Nrd1p-Nab3p and Ctk1p are direct or indirect cannot be determined from our experiments. It is possible, but not likely, that these proteins are regulated directly by CTDK-I phosphorylation. Deletion of *CTK1* did not significantly change the level of radioactive phosphate labeling of Nab3p *in vivo* (data not shown). Similarly, the ratio of phosphoisomers of Nrd1p is not changed in a *ctk1*Δ strain as judged by mobility in SDS-PAGE (data not shown). However, both of these assays would likely fail to detect a change in a single phosphorylation site of a multiply phosphorylated protein. Ctk1p is more likely to regulate the function of Nrd1p and Nab3p in an indirect manner. For example, changes in the phosphorylation pattern of the CTD may alter the interaction of Nrd1p and Nab3p with the transcription apparatus.

A possible mechanism for the control of RNA synthesis by the Nrd1p-Nab3p complex: Both *NAB3* and *NRD1* were isolated in independent genetic screens as suppressors of (pre-)mRNA accumulation phenotypes (Sugimoto *et al.* 1995; Steinmetz and Brow 1996). Physical and genetic interactions among Nrd1p, Nab3p, and RNA pol II described here suggest a potential mechanism by which Nrd1p and Nab3p function together at the interface between transcription and pre-mRNA processing. In the generalized model proposed here, Nrd1p and Nab3p, perhaps in association with other hnRNPs or RNA-processing factors, form a complex that binds to specific *cis*-acting sites in nascent transcripts. The Nrd1p-Nab3p complex then interacts with pol II, leading to pausing or termination. Alternatively, the Nrd1p-Nab3p complex may be bound to the elongating polymerase early in the transcription cycle so that it can monitor the nascent transcript. The interaction of Nrd1p and Nab3p in a complex may allow a greater range of specificity and affinity for RNA targets than could be achieved by either protein alone, enabling a form of combinatorial control at the level of transcript elongation. Genetic evidence indicates that CTDK-I functions to oppose the activity of the Nrd1p-Nab3p complex. CTDK-I may alleviate blocks to transcript elongation by directly dissociating the Nrd1p-Nab3p RNA complex, or by disrupting the pol II-Nrd1p-Nab3p complex by changing the CTD phosphorylation pattern. This model is summarized in Figure 9B.

Previous studies showing that truncated products of the *nrd1-1* and *nrd1-2* nonsense mutant alleles can interfere with pre-mRNA downregulation by full-length Nrd1p (Steinmetz and Brow 1998) are consistent with this model. It was proposed that these truncated products, predicted to include amino acid residues 1–241 and 1–285, respectively, compete with full-length Nrd1p for binding to the CTD. It is now evident that these truncated products also contain the Nab3p interaction domain, and thus may also compete with intact Nrd1p for Nab3p interactions. A role for Nab3p in Nrd1p-dependent downregulation of pre-mRNA containing the U6R* RNA element could account for the observation that additional sequences outside of the 43-nt segment of U6R* shown to bind to Nrd1p *in vitro* are required for downregulation *in vivo*. These additional sequences may contain elements that interact productively with Nab3p, and the combined action of Nrd1p and Nab3p bound to RNA ligands may be required for downregulation.

Recently, mammalian complexes have been described that negatively affect transcript elongation *in vitro*. These negative factors include the negative elongation factor NELF (Yamaguchi *et al.* 1999) and the DRB

sensitivity-inducing factor (DSIF; Hartzog *et al.* 1998; Wada *et al.* 1998a,b). The only known subunit of NELF is RD, a 43.2-kD protein, which, like Nrd1p, contains a single RRM and a motif rich in alternating positive/negative dipeptides (RD). DSIF is comprised of homologs of yeast Spt4p and Spt5p that interact with each other and pol II (Hartzog *et al.* 1998; Wada *et al.* 1998a). Interestingly, the affects of DSIF and NELF can be counteracted by P-TEFb, a kinase/cyclin pair (Cdk9/cyclin T) that is closely related to CTDK-I (Zhu *et al.* 1997; Peng *et al.* 1998b; Wei *et al.* 1998). CTDK-I and P-TEFb share amino acid homology in their kinase subunits, and both phosphorylate the CTD and stimulate elongation *in vitro* (Sterner *et al.* 1995; Lee and Greenleaf 1997; Zhu *et al.* 1997; Peng *et al.* 1998a,b; Wei *et al.* 1998). While the exact mechanism of NELF/DSIF and P-TEFb remains to be elucidated, the model we are proposing for Nrd1p-Nab3p is similar to that described for DSIF/NELF (Peng *et al.* 1998a; Wada *et al.* 1998b; Yamaguchi *et al.* 1999).

While it is unclear whether or not NELF is gene specific, in our model, Nrd1p-Nab3p acts as a gene-specific regulator of transcription. The RNA-binding specificity of Nrd1p has been demonstrated *in vitro* (Steinmetz and Brow 1998). The binding specificity of Nab3p is not known, but *nab3* mutants have been shown to have gene-specific expression defects (Wilson *et al.* 1994; Sugimoto *et al.* 1995). How many genes are regulated by Nrd1p-Nab3p is also not known, but neither Nrd1p nor Nab3p is abundant, suggesting a small number of essential targets.

To date, the functions attributed to yeast hnRNPs have included involvement in 3′ processing, mRNA transport, and regulation of the degradation of mRNA. Here we have demonstrated genetic and physical interactions between nuclear pre-mRNA-binding proteins and the CTD of pol II. The present work represents a starting point to examine a potential role for yeast hnRNPs in the regulation of the synthesis of pol II transcripts.

We thank Debbie Kuehn (Johns Hopkins) for assistance in the early stages of this work, Priscilla Non (University of Florida) for several yeast strains and expert technical assistance, and Phil James (University of Wisconsin) for supplying the strain, plasmids, and libraries for the yeast two-hybrid experiment. This work was supported by grants from the National Science Foundation (J.L.C., M.C.B. 9723965) and National Institutes of Health (M.S.S., GM46272; D.A.B., GM44665).

LITERATURE CITED

Ausubel, F. M., R. Brent, R. E. Kingston, D. D. Moore, J. G. Seidman *et al.* (Editors), 1995 *Current Protocols in Molecular Biology*. John Wiley & Sons, New York.

Bender, A., and J. R. Pringle, 1991 Use of a screen for synthetic lethal and multicopy suppressee mutants to identify two new genes involved in morphogenesis in *Saccharomyces cerevisiae*. Mol. Cell. Biol. **11:** 1295–1305.

Boeke, J. D., F. LaCroute and G. R. Fink, 1984 A positive selection for mutants lacking orotidine-5′-phosphate decarboxylase activity in yeast: 5-fluoro-orotic acid resistance. Mol. Gen. Genet. **197:** 345–346.

Brachmann, C. B., A. Davies, G. J. Cost, E. Caputo, J. Li *et al.* 1998 Designer deletion strains derived from *Saccharomyces cerevisiae* S288C: a useful set of strains and plasmids for PCR-mediated gene disruption and other applications. Yeast **14:** 115–132.

Caceres, J. F., G. R. Screaton and A. R. Krainer, 1998 A specific subset of SR proteins shuttles continuously between the nucleus and the cytoplasm. Genes Dev. **12:** 55–66.

Cho, E. J., T. Takagi, C. R. Moore and S. Buratowski, 1997 mRNA capping enzyme is recruited to the transcription complex by phosphorylation of the RNA polymerase II carboxy-terminal domain. Genes Dev. **11:** 3319–3326.

Cho, E. J., C. R. Rodriquez, T. Takagi and S. Buratowski, 1998 Allosteric interactions between capping enzyme subunits and the RNA polymerase II carboxy-terminal domain. Genes Dev. **12:** 3482–3487.

Christianson, T. W., R. S. Sikorski, M. Dante, J. H. Shero and P. Hieter, 1992 Multifunctional yeast high-copy-number shuttle vectors. Gene **110:** 119–122.

Connelly, C., and P. Hieter, 1996 Budding yeast SKP1 encodes an evolutionarily conserved kinetochore protein required for cell cycle progression. Cell **86:** 275–285.

Corden, J. L., and M. Patturajan, 1997 A CTD function linking transcription to splicing. Trends Biochem. Sci. **22:** 413–416.

Dahmus, M. E., 1996 Reversible phosphorylation of the C-terminal domain of RNA polymerase II. J. Biol. Chem. **271:** 19009–19012.

Fu, X. D., 1995 The superfamily of arginine/serine-rich splicing factors. RNA **1:** 663–680.

Guldener, U., S. Heck, T. Fielder, J. Beinhauer and J. H. Hegemann, 1996 A new efficient gene disruption cassette for repeated use in budding yeast. Nucleic Acids Res. **24:** 2519–2524.

Harlow, E., and D. Lane (Editors), 1988 *Antibodies: A Laboratory Manual*. Cold Spring Harbor Laboratory, Cold Spring Harbor, NY.

Hartzog, G. A., T. Wada, H. Handa and F. Winston, 1998 Evidence that Spt4, Spt5, and Spt6 control transcription elongation by RNA polymerase II in *Saccharomyces cerevisiae*. Genes Dev. **12:** 357–369.

Henry, M., C. Z. Borland, M. Bossie and P. A. Silver, 1996 Potential RNA binding proteins in *Saccharomyces cerevisiae* identified as suppressors of temperature-sensitive mutations in *NPL3*. Genetics **142:** 103–115.

Hirose, Y., and J. L. Manley, 1998 RNA polymerase II is an essential mRNA polyadenylation factor. Nature **395:** 93–96.

Hirose, Y., R. Tacke and J. L. Manley, 1999 Phosphorylated RNA polymerase II stimulates pre-mRNA splicing. Genes Dev. **13:** 1234–1239.

Ho, C. K., and S. Shuman, 1999 Distinct roles for CTD ser-2 and ser-5 phosphorylation in the recruitment and allosteric activation of mammalian mRNA capping enzyme. Mol. Cell **3:** 405–411.

Ho, C. K., V. Sriskanda, S. McCracken, D. Bentley, B. Schwer *et al.* 1998 The guanylyltransferase domain of mammalian mRNA capping enzyme binds to the phosphorylated carboxyl-terminal domain of RNA polymerase II. J. Biol. Chem. **273:** 9577–9585.

James, P., J. Halladay and E. A. Craig, 1996 Genomic libraries and a host strain designed for highly efficient two-hybrid selection in yeast. Genetics **144:** 1425–1436.

Kessler, M. M., M. F. Henry, E. Shen, J. Zhao, S. Gross *et al.* 1997 Hrp1, a sequence-specific RNA-binding protein that shuttles between the nucleus and the cytoplasm, is required for mRNA 3′-end formation in yeast. Genes Dev. **11:** 2545–2556.

Kim, E., L. Du, D. B. Bregman and S. L. Warren, 1997 Splicing factors associate with hyperphosphorylated RNA polymerase II in the absence of pre-mRNA. J. Cell Biol. **136:** 19–28.

Krecic, A. M., and M. S. Swanson, 1999 hnRNP complexes: composition, structure, and function. Curr. Opin. Cell Biol. **11:** 363–371.

Lee, J. M., and A. L. Greenleaf, 1989 A protein kinase that phosphorylates the C-terminal repeat domain of the largest subunit of RNA polymerase II. Proc. Natl. Acad. Sci. USA **86:** 3624–3628.

Lee, J. M., and A. L. Greenleaf, 1991 CTD kinase large subunit is encoded by CTK1, a gene required for normal growth of *Saccharomyces cerevisiae*. Gene Expr. **1:** 149–167.

Lee, J. M., and A. L. Greenleaf, 1997 Modulation of RNA polymer-

ase II elongation efficiency by C-terminal heptapeptide repeat domain kinase I. J. Biol. Chem. **272:** 10990–10993.

Lee, M. S., M. Henry and P. A. Silver, 1996 A protein that shuttles between the nucleus and the cytoplasm is an important mediator of RNA export. Genes Dev. **10:** 1233–1246.

McCracken, S., N. Fong, E. Rosonia, K. Yankulov, G. Brothers *et al.* 1997a 5′ capping enzymes are targeted to pre-mRNA by binding to the phosphorylated C-terminal domain of RNA polymerase II. Genes Dev. **11:** 3306–3318.

McCracken, S., N. Fong, K. Yankulov, S. Ballantyne, G. Pan *et al.* 1997b The C-terminal domain of RNA polymerase II couples mRNA processing to transcription. Nature **385:** 357–361.

Meisels, E., O. Gileadi and J. L. Corden, 1995 Partial truncation of the yeast RNA polymerase II carboxyl-terminal domain preferentially reduces expression of glycolytic genes. J. Biol. Chem. **270:** 31255–31261.

Minvielle-Sebastia, L., K. Beyer, A. M. Krecic, R. E. Hector, M. S. Swanson *et al.* 1998 Control of cleavage site selection during mRNA 3′ end formation by a single yeast hnRNP. EMBO J. **17:** 7454–7468.

Misteli, T., and D. L. Spector, 1999 RNA polymerase II targets pre-mRNA splicing factors to transcription sites in vivo. Mol. Cell **3:** 697–705.

Mortillaro, M. J., B. J. Blencowe, X. Wei, H. Nakayasu, L. Du *et al.* 1996 A hyperphosphorylated form of the large subunit of RNA polymerase II is associated with splicing complexes and the nuclear matrix. Proc. Natl. Acad. Sci. USA **93:** 8253–8257.

Muhlrad, D., R. Hunter and R. Parker, 1992 A rapid method for localized mutagenesis of yeast genes. Yeast **8:** 79–82.

Myer, V. E., and R. A. Young, 1998 RNA polymerase II holoenzymes and subcomplexes. J. Biol. Chem. **273:** 27757–27760.

Nonet, M., D. Sweetser and R. A. Young, 1987 Functional redundancy and structural polymorphism in the large subunit of RNA polymerase II. Cell **50:** 909–915.

Patturajan, M., R. J. Schulte, B. M. Sefton, R. Berezney, M. Vincent *et al.* 1998a Growth-related changes in phosphorylation of yeast RNA polymerase II. J. Biol. Chem. **273:** 4689–4694.

Patturajan, M., X. Y. Wei, R. Berezney and J. L. Corden, 1998b A nuclear matrix protein interacts with the phosphorylated C-terminal domain of RNA polymerase II. Mol. Cell. Biol.**18:** 2406–2415.

Peng, J., M. Liu, J. Marion, Y. Zhu and D. H. Price, 1998a RNA polymerase II elongation control. Cold Spring Harbor Symp. Quant. Biol. **63:** 365–370.

Peng, J., Y. Zhu, J. T. Milton and D. H. Price, 1998b Identification of multiple cyclin subunits of human P-TEFb. Genes Dev. **12:**755–762.

Pillutla, R. C., Z. Yue, E. Maldonado and A. J. Shatkin, 1998 Recombinant human mRNA cap methyltransferase binds capping enzyme/RNA polymerase IIo complexes. J. Biol. Chem. **273:** 21443–21446.

Rose, M. D., F. Winston and P. Hieter, 1990 *Methods in Yeast Genetics: A Laboratory Course Manual.* Cold Spring Harbor Laboratory Press, Cold Spring Harbor, NY.

Scafe, C., M. Nonet and R. A. Young, 1990 RNA polymerase II mutants defective in transcription of a subset of genes. Mol. Cell. Biol. **10:** 1010–1016.

Schiestl, R. H., and R. D. Gietz, 1989 High efficiency transformation of intact yeast cells using single stranded nucleic acids as a carrier. Curr. Genet. **16:** 339–346.

Sikorski, R. S., and P. Hieter, 1989 A system of shuttle vectors and yeast host strains designed for efficient manipulation of DNA in *Saccharomyces cerevisiae.* Genetics **122:** 19–27.

Siomi, H., and G. Dreyfuss, 1997 RNA-binding proteins as regulators of gene expression. Curr. Opin. Genet. Dev. **7:** 345–353.

Steinmetz, E. J., 1997 Pre-mRNA processing and the CTD of RNA polymerase II: the tail that wags the dog? Cell **89:** 491–494.

Steinmetz, E. J., and D. A. Brow, 1996 Repression of gene expression by an exogenous sequence element acting in concert with a heterogeneous nuclear ribonucleoprotein-like protein, Nrd1, and the putative helicase Sen1. Mol. Cell. Biol. **16:** 6993–7003.

Steinmetz, E. J., and D. A. Brow, 1998 Control of pre–mRNA accumulation by the essential yeast protein Nrd1 requires high-affinity transcript binding and a domain implicated in RNA polymerase II association. Proc. Natl. Acad. Sci. USA **95:** 6699–6704.

Sterner, D. E., J. M. Lee, S. E. Hardin and A. L. Greenleaf, 1995 The yeast carboxyl-terminal repeat domain kinase CTDK-I is a divergent cyclin-cyclin-dependent kinase complex. Mol. Cell. Biol. **15:** 5716–5724.

Sugimoto, K., K. Matsumoto, R. D. Kornberg, S. I. Reed and C. Wittenberg, 1995 Dosage suppressors of the dominant G1 cyclin mutant CLN3-2: identification of a yeast gene encoding a putative RNA/ssDNA binding protein. Mol. Gen. Genet. **248:** 712–718.

Tyers, M., G. Tokiwa, R. Nash and B. Futcher, 1992 The Cln3-Cdc28 kinase complex of S. cerevisiae is regulated by proteolysis and phosphorylation. EMBO J. **11:** 1773–1784.

Wada, T., T. Takagi, Y. Yamaguchi, A. Ferdous, T. Imai *et al.* 1998a DSIF, a novel transcription elongation factor that regulates RNA polymerase II processivity, is composed of human Spt4 and Spt5 homologs. Genes Dev. **12:** 343–356.

Wada, T., T. Takagi, Y. Yamaguchi, D. Watanabe and H. Handa, 1998b Evidence that P-TEFb alleviates the negative effect of DSIF on RNA polymerase II-dependent transcription in vitro. EMBO J. **17:** 7395–7403.

Wei, P., M. E. Garber, S. Fang, W. H. Fischer and K. A. Jones, 1998 A novel CDK9-associated C-type cyclin interacts directly with HIV-1 tat and mediates its high-affinity, loop-specific binding to TAR RNA. Cell **92:** 451–462.

West, M. L., and J. L. Corden, 1995 Construction and analysis of yeast RNA polymerase II CTD deletion and substitution mutants. Genetics **140:** 1223–1233.

Wilson, I. A., H. L. Niman, R. A. Houghten, A. R. Cherenson, M. L. Connolly *et al.* 1984 The structure of an antigenic determinant in a protein. Cell **37:** 767–778.

Wilson, S. M., K. V. Datar, M. R. Paddy, J. R. Swedlow and M. S. Swanson, 1994 Characterization of nuclear polyadenylated RNA-binding proteins in *Saccharomyces cerevisiae.* J. Cell Biol. **127:** 1173–1184.

Yamaguchi, Y., T. Takagi, T. Wada, K. Yano, A. Furuya *et al.* 1999 NELF, a multisubunit complex containing RD, cooperates with DSIF to repress RNA polymerase II elongation. Cell **97:** 41–51.

Yue, Z., E. Maldonado, R. Pillutla, H. Cho, D. Reinberg *et al.* 1997 Mammalian capping enzyme complements mutant *Saccharomyces cerevisiae* lacking mRNA guanylyltransferase and selectively binds the elongating form of RNA polymerase II. Proc. Natl. Acad. Sci. USA **94:** 12898–12903.

Yuryev, A., and J. L. Corden, 1996 Suppression analysis reveals a functional difference between the serines in positions two and five in the consensus sequence of the C-terminal domain of yeast RNA polymerase II. Genetics **143:** 661–671.

Yuryev, A., M. Patturajan, Y. Litingtung, R. V. Joshi, C. Gentile *et al.* 1996 The C-terminal domain of the largest subunit of RNA polymerase II interacts with a novel set of serine/arginine-rich proteins. Proc. Natl. Acad. Sci. USA **93:** 6975–6980.

Zhu, Y., T. Pe'ery, J. Peng, Y. Ramanathan, N. Marshall, *et al.* 1997 Transcription elongation factor P-TEFb is required for HIV-1 Tat transactivation in vitro. Genes Dev. **11:** 2622–2632.

Communicating editor: F. Winston